Absence of singular stretching of interacting vortex filaments

Sahand Hormoz† and Michael P. Brenner

School of Engineering and Applied Sciences, and Kavli Institute for Bionano Science and Technology, Harvard University, Cambridge, MA 02138, USA

A promising mechanism for generating a finite-time singularity in the incompressible Euler equations is the stretching of vortex filaments. Here, we argue that interacting vortex filaments cannot generate a singularity by analysing the asymptotic dynamics of their collapse. We use the separation of the dynamics of the filament shape, from that of its core, to derive constraints that must be satisfied for a singular solution to remain self-consistent uniformly in time. Our only assumption is that the length scales characterizing filament shape obey scaling laws set by the dimension of circulation as the singularity is approached. The core radius necessarily evolves on a different length scale. We show that a self-similar ansatz for the filament shapes cannot induce singular stretching, due to the logarithmic prefactor in the self-interaction term for the filaments. More generally, there is an antagonistic relationship between the stretching rate of the filaments and the requirement that the radius of curvature of filament shape obeys the dimensional scaling laws. This suggests that it is unlikely that solutions in which the core radii vanish sufficiently fast to maintain the filament approximation exist.

---

1. Introduction

There has been much effort, both numerical and analytical, to determine whether smooth initial conditions of the three-dimensional Euler equation can develop singularities in finite time (Leray 1934; Majda & Bertozzi 2001; Childress 2008; Constantin 2008; Gibbon 2008). Vortex stretching creates a non-local source term in the vorticity equation that scales quadratically with vorticity. This nonlinearity creates the possibility of a singularity in which vorticity diverges as $(t^* - t)^{-1}$, though non-locality creates uncertainty about whether this blowup can be realized. Beale, Kato & Majda (1984) showed that any solution without a blowup in the time integral of the maximum vorticity is smooth, thus demonstrating that a vorticity divergence must be at least as strong as this simple argument suggests. More recent results have established that, if the direction of the vorticity varies too smoothly in space (Constantin 2008) or if vortex lines have sufficient regularity (Deng, Hou & Yu 2006; Hou & Li 2006), then singularities are not possible.

On the numerical side there have been repeated efforts to determine whether a particular initial condition could lead to a singularity, starting with the original study of the Taylor–Green vortex (Taylor & Green 1937; Morf, Orszag & Frisch 1980;

† Email address for correspondence: sahand.hormoz@gmail.com

Meiron *et al.* 1983). In essentially every case, an initial report of numerical evidence for a singular solution is followed, after a typical 5–10 year delay, with higher-resolution simulations arguing against a singularity for the initial condition in question – see the table in Gibbon (2008). It seems reasonable to conclude from these studies that singular solutions do not form from generic initial data; thus, if singular solutions to the Euler equation exist, they are likely to have either a small basin of attraction or to be unstable. In either case, finding a singular solution requires systematic search.

The present study was undertaken with the goal of systematically searching for (potentially unstable) singular solutions, where the initial conditions are vortex filaments (Morf *et al.* 1980; Siggia 1985; Pumir & Siggia 1987, 1990; Kerr 1993; Klein & Majda 1993; Klein, Majda & Damodaran 1995; Pelz 1997; Childress 2008; Kimura 2010). Vortex filaments are especially promising initial data, since they can potentially survive the addition of viscosity and generate singular solutions to the Navier–Stokes equations. It has long been known that, when two vortex filaments come together, there is significant vorticity amplification, with the vortex lines developing a sharp kink. However, numerical simulations of specific initial conditions have shown that when two antiparallel vortices come together, their cores flatten significantly, halting vorticity amplification.

We aimed to discover whether there exist initial conditions of collections of vortex filaments that evade strong core deformation during a collision: this requires that the core radius σ remains smaller than any length scale associated with the vortex filament. Such configurations, e.g. those involving simultaneous collision of multiple vortex filaments, are likely to be unstable. Since the dynamics of filament shape involves the dimensional circulation Γ, it is natural that any length scale associated with the filament shape should satisfy $\ell(t) = \sqrt{\Gamma(t^* - t)}$. We show that surprisingly the core radius σ has a different non-universal exponent that depends on the *shape* of the filaments. The requirement that this exponent is larger than $1/2$ sets a precise dynamical criterion for core deformation to be avoided. We demonstrate that self-similar solutions for the filament shape cannot satisfy this criterion, due to a specific feature of the vortex interaction law, the logarithmic prefactor to the binormal law (the first term in (2.2) below). More generally, we demonstrate that there is an antagonistic relationship between the stretching rate of the filaments and the requirement that the radius of curvature of filament shape obeys the dimensional scaling laws. Solutions in which the core radius shrinks fast enough for self-consistency appear to violate the dimensional scaling law for the filament curvature.

It is worth emphasizing that the solutions we construct are not strictly self-similar: either the length scale characterizing the filament evolves differently than that characterizing the core, or there is explicit time dependence (depending on the logarithm of the time to the singularity) as the singularity is approached. Indeed, it has already been proven that strictly self-similar solutions to the Euler equations cannot be singular under certain integrability conditions of the vorticity profile, which include finite-energy vortex filaments (Chae 2007, 2010).

Although our results are not mathematically rigorous, they are asymptotically self-consistent, and appear to rule out an appealing class of initial data (interacting vortex filaments) for forming singularities in the Euler equations.

2. Formulation

Vortex filaments approximate the velocity field produced by vortex tubes, in which the vorticity distribution is limited to a tube of radius σ (Schwarz 1985; Saffman

1992). When the radius of curvature of the filament is much larger than the core radius, the velocity field produced by each vortex filament is given by the Biot–Savart law,

$$\boldsymbol{v}(\boldsymbol{r}_0) = -\frac{\Gamma}{4\pi} \int \frac{(\boldsymbol{r}_0 - \boldsymbol{r}(s)) \times \boldsymbol{t}(s)}{|\boldsymbol{r}_0 - \boldsymbol{r}(s)|^3} \, ds, \tag{2.1}$$

with Γ the circulation of the filament, $\boldsymbol{r}(s)$ the shape of the filament, $\boldsymbol{t}$ the tangent vector and $\boldsymbol{r}_0$ the location at which the velocity field is measured. The approximation accurately captures the interaction of multiple filaments with each other, as long as the core radius of each filament is much smaller than the inter-filament distance.

If $\boldsymbol{r}_0$ is on the axis of the vortex filament, the Biot–Savart law (2.1) is (logarithmically) singular. This is evident if $\boldsymbol{r}(s)$ is expanded to second-order around $\boldsymbol{r}_0$: $\boldsymbol{r}(s) = \boldsymbol{r}_0 + s\boldsymbol{t}_0 + \frac{1}{2}s^2\kappa\boldsymbol{n}_0 + O(s^3)$, where $\boldsymbol{t}_0$ and $\boldsymbol{n}_0$ are the orthogonal tangential and normal vectors at $\boldsymbol{r}_0$, respectively, and $\kappa = r_c^{-1}$ the curvature of the filament. The expansion is valid up to the length scale characterizing the shape of the filament, namely r_c in this case. Plugging this into (2.1), and evaluating the local contribution to the velocity (small s), gives $\boldsymbol{v} \sim \int_0^{r_c}(1/s)\,ds$, which is logarithmically divergent because of its lower bound.

This divergence is cut off by setting the lower bound as the finite vortex core size σ, yielding the regularized Biot–Savart law (Saffman & Baker 1979; Schwarz 1985)

$$\boldsymbol{v}(\boldsymbol{r}_0) = -\frac{\Gamma}{4\pi} \log\left(\frac{r_c}{\sigma}\right)\kappa\boldsymbol{b} - \frac{\Gamma}{4\pi} \int' \frac{(\boldsymbol{r}_0 - \boldsymbol{r}(s)) \times \boldsymbol{t}(s)}{|\boldsymbol{r}_0 - \boldsymbol{r}(s)|^3} \, ds. \tag{2.2}$$

Here, $\boldsymbol{b} = \boldsymbol{t} \times \boldsymbol{n}$ is the binormal vector, and $\int'$ the regularized integral that runs along the non-local part of the filament. Note that the dynamics of the shape of the vortex filament depends very weakly (logarithmically) on the dynamics of the core (σ); hence the two problems are naturally decoupled.

The large fluid shears associated with colliding vortex filaments can cause dramatic changes to both the shape of the filament and the shape of the core. For the vortex filament approximation to remain an accurate description of a collision, the core radii of the vortex filaments must remain smaller than the length scales characterizing the vortices uniformly in time; this means that the radius of the tubes must shrink more quickly than the distance between colliding filaments.

The essence of our approach for searching for putative singularities of the Euler equation is to start with initial conditions for which the vortex filament approximation is valid, and then to determine whether there are solutions in which a finite-time singularity exists and which the filament approximation remains valid uniformly in time. For this to happen, the core radius σ must remain smaller than any length scale associated with the vortex filament. We adopt a simplified, but reasonable, model for the dynamics of the core, that the core radius evolves to satisfy volume conservation: if s measures arclength along a filament, with the original filament parametrized by α, then s_α measures the stretching of a filament. We then have that

$$\sigma^2 = \frac{\sigma_0^2}{s_\alpha}. \tag{2.3}$$

In general, if the dynamics of the vortex core is decomposed into a local coordinate system,

$$\frac{d\boldsymbol{r}}{dt} = W\boldsymbol{t} + U\boldsymbol{n} + V\boldsymbol{b}, \tag{2.4}$$

where $\boldsymbol{n}$, $\boldsymbol{t}$ and $\boldsymbol{b}$ are respectively the normal, tangent and binormal vectors, then the stretching of the filament evolves according to

$$\frac{\mathrm{d}s_\alpha}{\mathrm{d}t} = \left(\frac{\mathrm{d}\boldsymbol{v}}{\mathrm{d}s}\cdot\boldsymbol{t}\right)s_\alpha = \frac{\mathrm{d}W}{\mathrm{d}s}s_\alpha - U\kappa s_\alpha. \tag{2.5}$$

The first term in (2.5) is the stretching of the filament due to local shear, whereas the second term is due to motion in the normal direction. Since the circulation is constant, the local vorticity in the vortex filament is given by $\omega = \Gamma\left(\pi\sigma^2\right)^{-1} \propto \Gamma s_\alpha$. Hence, a diverging vorticity is equivalent to a diverging s_α.

3. Numerical simulations

We begin by simulating (2.2) and (2.5) numerically. The calculations of (2.2) are carried out by treating the local contribution implicitly, with a second-order Crank–Nicolson scheme, and the non-local one explicitly. The equation for the stretching rate (2.5) is solved explicitly, evaluating the local normal and tangential velocities on each vortex filament from the Biot–Savart equation (2.1). Moreover, to resolve any singular events with sufficient accuracy, we implement a dynamic remeshing scheme for the grid points along the filaments. A fixed total of $N = 800$ grid points are used for each filament. At each time step, the separation distance between the points is varied as a function of the inter-filament separation distance and the local curvature. Close to the singularity, roughly 25 % of the points are bunched at the tip (and infinitesimal distance along the filament) with separation distance between adjacent grid points comparable to the filament separation distance and radius of curvature, thereby properly resolving the shape (for more details see the supplementary material available at http://dx.doi.org/10.1017/jfm.2012.270).

We choose the initial condition introduced by Kerr (1993) for two antiparallel vortex filaments; the advantage of this initial condition is that there have been two independent efforts (Kerr 1993; Hou & Li 2006) to simulate the resulting dynamics with the full Euler equations, so this provides an excellent basis for comparison to our approximate solution. It should be emphasized that the majority of the vorticity amplification in the full Euler equations for this initial condition comes about after there has been significant flattening of the filament core, namely in the regime after our approximations apply.

Figures 1 and 2 show the results of the vortex filament simulation. Figure 1(*a*) shows several snapshots of the shapes of the filaments: the two filaments approach each other, driven by the drifts in the binormal direction from the local term in (2.2). Within the present approximation, the two vortex filaments collide in finite time. Such singular collapse of vortex filament models have been previously observed in theoretical studies (Klein *et al.* 1995) and even in experiments on quantum vortices (Paoletti *et al.* 2008; Paoletti, Fisher & Lathrop 2010).

Figure 1(*b*) shows the minimum separation between the two filaments as a function of time; this distance vanishes as $(t^* - t)^{1/2}$, where t^* is the time of filament collision. Figure 1(*c*) shows the time dependence of the filament radius during this process; during the five-order-of-magnitude decrease in the inter-filament distance, the core radius decreases by only a factor of two. Equation (2.3) then implies a fourfold increase in s_α, and hence the vorticity. The rate of decrease of the core with time to the singularity (figure 1*c*) is much slower than the approach rate of the filaments to each other.
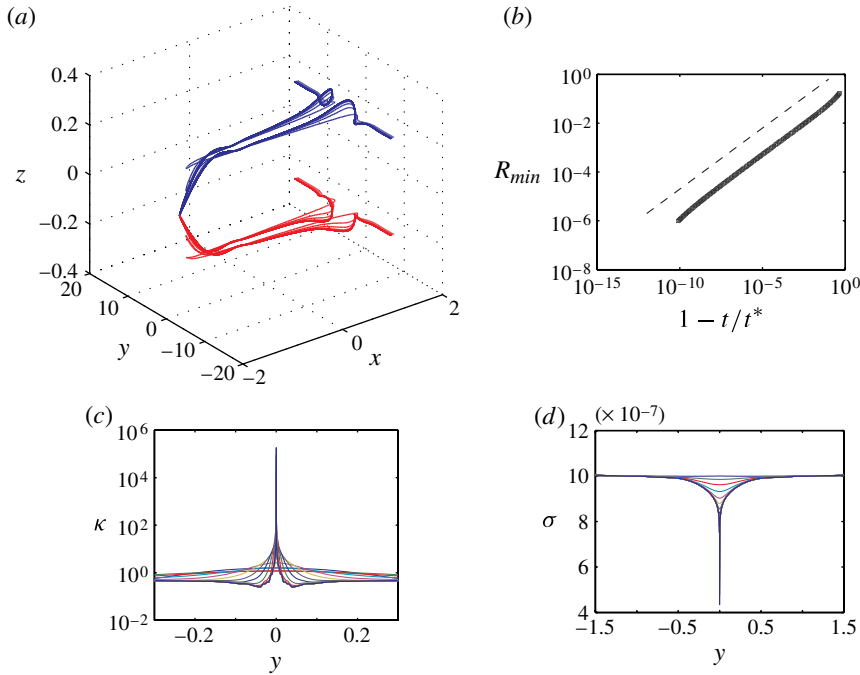
FIGURE 1. (Colour online) Numerical simulation of (2.2) and (2.5) with the Kerr initial conditions ($\Gamma_1 = -\Gamma_2 = 1$, $\sigma_0 = 10^{-6}$). (*a*) Filament shapes; many time steps superimposed. The first five time steps in units of $1 - t/t^*$ are 9.4×10^{-1}, 4.9×10^{-1}, 2.4×10^{-1}, 8.6×10^{-2} and 2.7×10^{-2} and the last time step is 1.2×10^{-10}. The initially flat filaments bend inwards as their tips get closer. (*b*) The power-law scaling of the minimum separation distance between the filaments and time to singularity. The dashed line has slope 0.5. The separation distance decreases by five orders of magnitude. (*c*) Curvature κ as a function of y coordinate for the same time steps as in (*a*). Curvature at the tip of the filaments increases by five orders of magnitude. (*d*) The core radius σ as a function of y coordinate for the same time steps as in (*a*). At the tip ($y = 0$), the core radius only decreases by a factor of two during the approach, ruling out a self-consistent collapse.
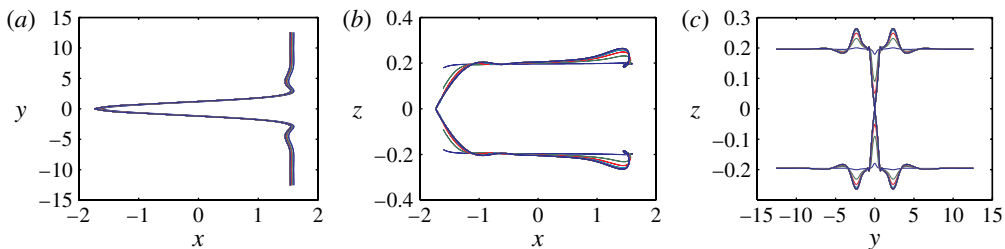

FIGURE 2. (Colour online) Projections of simulated filament shapes: (a, b, c) correspond respectively to *xy*, *xz* and *yz* projections of the filament shapes (for many superimposed time steps) numerically simulated using (2.2) and (2.5). The three-dimensional plot is shown in figure 1(*a*). The time steps are the same as in figure 1.

This scenario violates the Beale–Kato–Majda criterion (Beale *et al.* 1984), and correspondingly the vortex filament approximation is itself inconsistent. In the full

simulations of the Kerr initial condition, significant flattening of the core is observed at $t < t^*$. Note that, given the different asymptotic rates of the inter-filament separation distance and the core shrinkage rates (figure 1b,c), it follows that there exists no initial core radius for which this initial condition can be asymptotically consistent. If the initial core radius is smaller, the amount of vorticity amplification that occurs before the filament approximation is violated increases dramatically, but this never leads to a singularity.

4. The asymptotic solution and a consistency criterion

The simulations show that the vortex filament approximation fails before a singularity is reached. We now would like to examine whether this is generally true. Are there initial conditions for which two antiparallel filaments lead to a consistent solution? Does the answer change if the filaments are not antiparallel, i.e. the two filaments have different circulations?

To answer this, we need to develop an understanding of why the results of the simulations occur. The key idea is to realize that, in the asymptotic limit, the shape of the filaments follows the scaling law set by circulation to leading order, coupled to a core that follows its own scaling law. There are two length scales – one characterizing filament shape and the other size of the core – whose scaling exponents are coupled through the governing equations. We want to know if any asymptotic filament shape and dynamics (due to this coupling) can self-consistently stretch the core to generate a singularity.

From dimensional analysis (see e.g. Gutierrez, Rivas & Vega 2003) as well as the scaling laws computed numerically, to leading order, the characteristic length scales governing the filament shapes are $\ell_i(t) = \sqrt{|\Gamma_i|(t^* - t)}$, where $i = 1, 2$ denotes filament one or two with circulation Γ_i, and t^* the time of singularity. Throughout the remainder of this paper, we write all the equations for only the first filament $i = 1$, with the second filament obeying the complementary equation. The shapes of the filament then take the form

$$\boldsymbol{r}_1(s, t) = \ell_1(t)\boldsymbol{G}_1(\eta),\tag{4.1}$$

where $\eta = s/\ell_1(t)$, and s measures arclength along the filament. In general, $\boldsymbol{G}$ can have explicit time dependence; we neglect this now, but return to it at the end of the paper. Plugging the above similarity ansatz into (2.2) gives a set of coupled ordinary integro-differential equations for the shapes of the filament.

Although these equations are difficult to solve (but, see below), we can still use the asymptotic solution (4.1) to derive a condition for the self-consistency of the collapse of the core. We need to use the asymptotic solution in (2.5). The normal and tangential self-similar velocity components obey $U = u(\eta)\sqrt{|\Gamma_i|/(t^* - t)}$ and $W = w(\eta)\sqrt{|\Gamma_i|/(t^* - t)}$, whereas the curvature of the filament is given by $\kappa = k(\eta)/\sqrt{|\Gamma_i|(t^* - t)}$; hence, $U\kappa = u(\eta)k(\eta)/(t^* - t)$ and $W_s = w'(\eta)/(t^* - t)$. Here, $u(\eta)$, $k(\eta)$ and $w(\eta)$ are location-dependent prefactors, given by the solution of asymptotic equations. Putting this together in (2.5), we obtain that

$$\frac{\mathrm{d}s_\alpha}{\mathrm{d}t} = \frac{w'(\eta) - u(\eta)k(\eta)}{t^* - t}s_\alpha.\tag{4.2}$$

Hence, the stretching rate of the filament obeys a power law $s_\alpha \sim (t^* - t)^{-p(\eta)}$, with the position-dependent exponent $p(\eta)$ given by the asymptotic solution! Equation (2.3) then implies that the filament radius vanishes according to $\sigma \sim (t^* - t)^{p(\eta)/2}$. We

note that the observation that the prefactors in the asymptotic solutions for outer filaments control the power-law exponents for the core collapse was anticipated by Moffatt (2000), who studied the behaviour of inviscid vortex filaments under power-law diverging strains.

We therefore have arrived at a criterion for self-consistency of the collapsing filament solution: self-consistency requires that the filament radius decreases faster than the inter-filament separation, or $p > 1$. Indeed, since the vorticity scales with s_α, this is a realization of the Beale–Kato–Majda criterion (Beale *et al.* 1984) for vortex filaments. Recent rigorous theorems (Chae 2007) indicate that $p = 1$ is not allowed, since it would imply a solution where all length scales follow the same scaling law, namely $\sim \sqrt{t^* - t}$. Such finite-energy 'strictly' self-similar solutions cannot be singular (Chae 2007). Self-consistency condition $p > 1$ also satisfies the geometrical constraints of Constantin, Fefferman & Majda (1996) and bounds of Deng *et al.* (2006) for a singularity. Lastly, note that the self-consistency criterion justifies why in (2.2) the filament radius only modifies the local term (first term on the right-hand side). The filament radius becomes asymptotically negligible compared to the inter-filament separation distance, and need not be accounted for in the non-local contribution to the velocity. However, doing so would increase the accuracy of simulations where the self-consistency criterion does not hold (see e.g. Pumir & Siggia 1987).

5. Analysis

5.1. *Stretching and the asymptotic solution*

If we plug the similarity ansatz equation (4.1) into (2.2) we get an equation for the shape of the filament, namely

$$G_1 - \eta G_1' \approx \alpha \frac{\Gamma_1}{|\Gamma_1|} G_1' \times G_1'' - F[G], \tag{5.1}$$

where $\alpha = [1/(2\pi)] \ln(r_c/\sigma)$ is the self-interaction term, and $F[G]$ corresponds to the (shape-dependent) non-local integral term on the right-hand side of (2.2), discussed in more detail below.

We have used an approximate equality above because an important distinction must be made between the velocity field given by taking the time derivative of the self-similarity ansatz equation (4.1) on the left-hand side of (5.1), and the velocity computed from the full Biot–Savart law on the right-hand side. Mainly, the equality is only valid modulo the tangential component of the velocity field along the filaments. To clarity this further, we write down an explicit expression for each velocity field.

Taking the time derivative of (4.1) gives $\partial_t r_1 = -(|\Gamma_1|/2\ell_1)(G_1 - \eta G_1')$, which we define as the velocity field capturing changes in the *shape* of the filaments:

$$\frac{v_1^{shape}(s, t)}{l_1'(t)} = G_1(\eta) - \eta G_1'(\eta). \tag{5.2}$$

Since the similarity ansatz only captures the shape of the filaments, its time derivative, does not include velocity components that leave the shape unchanged, i.e. those tangent to the filaments. The above velocity field is not the physical velocity experienced by a fluid particle, but the velocity of a filament shape marker at arclength s. It should be expected then that this velocity field results in no stretching. We can

verify this explicitly by plugging (5.2) into the stretching equation (2.5):

$$\tilde{p}(\eta) = -\frac{1}{2}\left(\frac{\mathrm{d}}{\mathrm{d}\eta}[(\boldsymbol{G}_1 - \eta\boldsymbol{G}_1') \cdot \boldsymbol{G}_1'] - (\boldsymbol{G}_1 - \eta\boldsymbol{G}_1') \cdot \boldsymbol{G}_1''\right) = 0. \tag{5.3}$$

The full velocity field $\boldsymbol{v_1}$ computed from the Biot–Savart law on the right-hand side of (5.1) is the physical velocity experienced by a fluid particle, and can be thought of as the shape velocity field plus a tangential component. To show this explicitly, we fix a Lagrangian marker α along the filament and follow its motion. Initially, α is equivalent to the arclength parameter, $s(\alpha, t_0) = \alpha$. The velocity of the Lagrangian marker is given by

$$\boldsymbol{v_1}(r(\alpha, t), t) = \frac{\partial}{\partial t}[l_1(t)\boldsymbol{G}_1(\eta)]_\alpha = l_1'(t)[\boldsymbol{G}_1 - \eta\boldsymbol{G}_1'] + s_t(\alpha, t)\boldsymbol{G}_1', \tag{5.4}$$

where the partial derivative is taken for fixed α. The first term on the right-hand side is equal to $\boldsymbol{v}_1^{shape}$ in (5.2), and the second term corresponds to the velocity moving the particle along the filament. It is easy to show that the second term is the source of stretching:

$$\frac{\partial \boldsymbol{v}_1}{\partial s} \cdot \boldsymbol{t}_1 = \frac{\partial \alpha}{\partial s}\frac{\partial}{\partial \alpha}s_t(\alpha, t) = \frac{1}{s_\alpha}\frac{\partial s_\alpha}{\partial t}, \tag{5.5}$$

where we have used the fact that the α and t partial derivatives commute. The right-hand side of the above equation is exactly the expression for stretching discussed before (4.2).

It is clear, then, that to compute the filaments' stretching correctly, we need to use the full velocity field from the Biot–Savart kernel. Since the self-interaction term of the Biot–Savart kernel points along the binormal direction, it does not contribute to stretching. The only term left to consider is the non-local contribution, $F[\boldsymbol{G}]$. As we will show, this term is sensitively dependent on the curvature of the filaments $\boldsymbol{G}_1''$. To proceed, then, we first derive an explicit expression for $\boldsymbol{G}_1''$ from (5.1). However, as we noted, (5.1) is only an equality modulo the component of the velocity field tangent to the filaments. To get around this nuisance, we project out the tangential component by taking the cross-product of both sides of (5.1) with $\boldsymbol{G}_1'$. The first term on the right-hand side simplifies further using the vector identity $\boldsymbol{G}_1' \times \boldsymbol{G}_1' \times \boldsymbol{G}_1'' = \boldsymbol{G}_1'(\boldsymbol{G}_1' \cdot \boldsymbol{G}_1'') - \boldsymbol{G}_1''(\boldsymbol{G}_1' \cdot \boldsymbol{G}_1') = -\boldsymbol{G}_1''$, where in the last step we have used $|\boldsymbol{G}_1'| = 1$, or equivalently $\boldsymbol{G}_1' \cdot \boldsymbol{G}_1'' = 0$.

Thus $\boldsymbol{G}_1''$ using the explicit expression for the $F[\boldsymbol{G}]$ term in (5.1) is given by

$$\boldsymbol{G}_1''(\eta) = -\frac{|\Gamma_1|}{\alpha\Gamma_1}\boldsymbol{G}_1'(\eta)$$
$$\times \left(\boldsymbol{G}_1(\eta) - \frac{\Gamma_2\sqrt{|\Gamma_2|}}{2\pi\sqrt{|\Gamma_1|}}\int\frac{(\sqrt{|\Gamma_1|}\boldsymbol{G}_1(\eta) - \sqrt{|\Gamma_2|}\boldsymbol{G}_2(\zeta)) \times \boldsymbol{G}_2'(\zeta)}{|\sqrt{|\Gamma_1|}\boldsymbol{G}_1(\eta) - \sqrt{|\Gamma_2|}\boldsymbol{G}_2(\zeta)|^3}\,\mathrm{d}\zeta\right). \tag{5.6}$$

The integration runs along the length of the second filament and the non-local portion of the first filament, which can be thought of as another filament.

Note that the shape of the asymptotic solution has an explicit time dependence through the parameter $\alpha = (2\pi)^{-1}\log(r_c/\sigma)$. If we assume that $r_c/\sigma \to \infty$ as $t \to t^*$, so that the asymptotic solution is self-consistent, then $\alpha \to \infty$ as $t \to t^*$. Equation (5.6) then implies that, as the singularity is approached, $\boldsymbol{G}'' \to 0$; the filament curvature

in similarity space asymptotically vanishes. Note that the curvature in real space $|\boldsymbol{G}''|/l_1$ still diverges, albeit more slowly than $1/\sqrt{t^* - t}$. This assertion is only valid assuming that the non-local integral does not compensate for growth in α. The non-local contribution $F[\boldsymbol{G}]$ is bounded as $t \to t^*$, since it corresponds to the Biot–Savart integral over filaments with asymptotically fixed shape (time-independent integrand). If non-self-similar solutions exist, the integrand can be time-dependent, a point that we will return to later. Time dependence of the limits of this integral cannot compensate for any form of divergence in α, since to match any solution of (5.6) properly to an outer solution, the asymptotic limit $\eta \to \infty$ must satisfy $\boldsymbol{G} \sim \eta$. The contribution of a straight line to the Biot–Savart integral, even when extended to infinity, is always finite.

It is then permitted to replace the interaction integral in (5.6) with a (non-integral) interaction term of straight filaments. Fortunately, in the limit of approaching the singularity, this approximation becomes exact as the filaments become straight lines. The corrections to the local approximation are of the order $1/\alpha$ and vanish for a self-consistent singularity.

At any point η along the asymptotic solution, the integral in (5.6) is dominated by the point η_2 on the other filament, which minimizes $|\sqrt{\Gamma_1}\boldsymbol{G}_1(\eta) - \sqrt{\Gamma_2}\boldsymbol{G}_2(\eta_2)|$, i.e. the point of closest approach. The non-self velocity field then simplifies to

$$\boldsymbol{v}_1^{local} = -\frac{\Gamma_2}{2\pi\sqrt{t^* - t}} \frac{[\sqrt{|\Gamma_1|}\boldsymbol{G}_1(\eta) - \sqrt{|\Gamma_2|}\boldsymbol{G}_2(\eta_2)] \times \boldsymbol{G}_2'(\eta_2)}{|\sqrt{|\Gamma_1|}\boldsymbol{G}_1(\eta) - \sqrt{|\Gamma_2|}\boldsymbol{G}_2(\eta_2)|^2}. \tag{5.7}$$

Note that this approximation is similar to the heralded local induction approximation (Saffman & Baker 1979) or the nearly parallel filament approximation (Klein *et al.* 1995), with one important caveat: there is a non-local relationship between the positions that interact on the two filaments, given by the point of closest approach.

Now that we have an explicit expression for the full velocity field, we can calculate the actual stretching. Stretching is caused by the non-local contribution to the velocity, since local self-induced velocity points in the binormal direction and does not stretch. From (2.5), the stretching exponent p is given by

$$p(\eta) = \frac{\sqrt{t^* - t}}{\sqrt{|\Gamma_1|}} \left(\frac{\mathrm{d}\boldsymbol{v}_1^{local}}{\mathrm{d}\eta} \cdot \boldsymbol{G}_1'(\eta) \right). \tag{5.8}$$

Evaluating this expression at $\eta = 0$, which by definition corresponds to the closest point of the two filaments in similarity space where $\boldsymbol{G}_1(0) - \boldsymbol{G}_2(0)$ is perpendicular to $\boldsymbol{G}_1'(0)$ and $\boldsymbol{G}_2'(0)$, gives

$$p_1(\eta = 0) = -\frac{\Gamma_2}{2\pi\sqrt{|\Gamma_1|}} \frac{\sqrt{|\Gamma_1|}\boldsymbol{G}_1(0) - \sqrt{|\Gamma_2|}\boldsymbol{G}_2(0)}{|\sqrt{|\Gamma_1|}\boldsymbol{G}_1(0) - \sqrt{|\Gamma_2|}\boldsymbol{G}_2(0)|^2} \cdot \left(\boldsymbol{G}_2''(0)\frac{\mathrm{d}\eta_2}{\mathrm{d}\eta} \times \boldsymbol{G}_1'(0) \right). \tag{5.9}$$

The most important feature of this result is that $p(\eta = 0)$ *vanishes* in the limit of $\tau \to \infty$ because $\boldsymbol{G}''$ vanishes in this limit. Given the requirement of $p > 1$ for a self-consistent singular collapse, we have violated our assumption that $r_c/\sigma \to \infty$, resulting in a contradiction. This shows that singularities of pairs of vortex filaments cannot happen. We remark that the term $\mathrm{d}\eta_2/\mathrm{d}\eta$, capturing the asymmetry between the shape of the two filaments, remains regular because the circulations $\Gamma_{1,2}$ are always finite (see (5.10) below).

The essential reason for lack of any solution with singular stretching is that the rather slow (logarithmic) flattening out of the filaments eventually overcomes any

clever tricks with filament shapes that can be incorporated using initial conditions or unequal circulations.

5.2. *Evaluating the prefactor numerically*

It is possible to solve numerically for G and in turn p by going to higher order in (5.7). This is useful for evaluating the prefactors in (5.9). The dependence of η_2 on η follows from the fact that the line connecting the closest approach points should be perpendicular to the tangent vectors on the filaments, so that $G_2'(\eta_2) \cdot [\sqrt{\Gamma_1} G_1(\eta) - \sqrt{\Gamma_2} G_2(\eta_2)] = 0$. Differentiating this relationship gives

$$\frac{\mathrm{d}\eta_2}{\mathrm{d}\eta} = \frac{\sqrt{\dfrac{|\Gamma_1|}{|\Gamma_2|}} \, G_2'(\eta_2) \cdot G_1'(\eta)}{G_2''(\eta_2) \cdot \left(G_2(\eta_2) - \sqrt{\dfrac{|\Gamma_1|}{|\Gamma_2|}} \, G_1(\eta)\right) + |G_2'(\eta_2)|^2}. \tag{5.10}$$

The set of asymptotic equations for the filament shapes thus becomes a set of delay differential equations. The equations are initialized by selecting the two closest points on the filaments (denoted as $\eta = \eta_2 = 0$), specifying the magnitude of $G_1(0) - G_2(0)$, and vectors $G_1'(0)$ and $G_2'(0)$ perpendicular to $G_1(0) - G_2(0)$. The details of how to solve the resulting delayed ordinary differential equations (ODEs) are discussed in the supplementary material (text S1).

Figure 3 depicts two particular examples of the asymptotic solution for different values of α. Increasing α results in higher radius of curvature and filaments that resemble straight lines. Many asymptotic solutions are possible depending on the value of the circulations and the choice of initial conditions in similarity (η) space. These solutions describe the initial approach and sharpening of colliding vortex filaments, as occurs for example in recent experiments on vortex interactions in superfluid helium (Paoletti *et al.* 2008, 2010). Our method reveals a two-parameter family of asymptotic collision geometries: pyramidal structures described by angles dependent on the initial conditions. This contradicts the prediction of a universal (albeit pyramidal shape) collision geometry (de Waele & Aarts 1994). Refer to the supplementary material for an explicit demonstration of many possible asymptotic collapse geometries. Understanding the relationship between collision geometry and initial conditions in similarity space can potentially elucidate the signature of quantum turbulence. However, our results demonstrate that in general there exists no self-consistent singular stretching of two vortex filaments, for any asymptotic geometry – and hence at some point in the time evolution the core deformation will be significant and invalidate the assumptions underlying our solution.

6. Generalization

The argument of the previous section shows that a self-similar ansatz for the filament shape does not allow singular stretching, due to the intrinsic connection between the stretching rate and the curvature of the filament (5.9). For self-similar solutions, the filament curvature vanishes in time due to the self-interaction term of vortex filaments, and this forces the stretching rate also to vanish asymptotically. Indeed, this argument naturally generalizes to the self-similar collapse of multiple vortex filaments (e.g. Aref 1979) – in the same way as the two-filament case described above, the logarithmic self-interaction term again naturally causes the curvature of each filament to vanish asymptotically, and this in turn limits the filament stretching rate, making a self-consistent singular solution impossible.
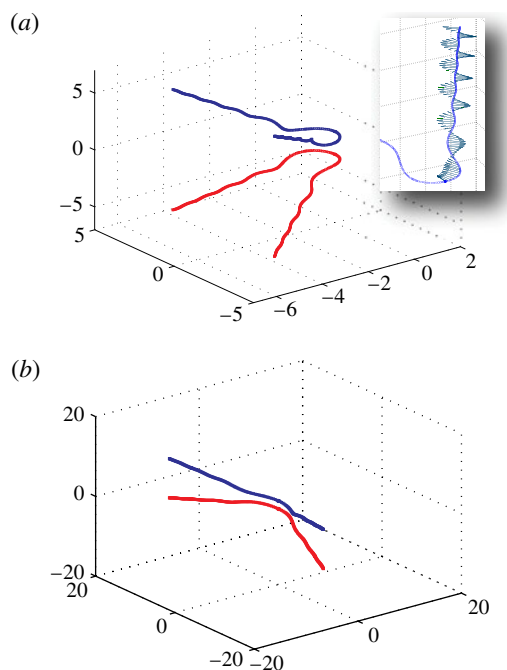
FIGURE 3. (Colour online) Numerical solution of the asymptotic ODE using local approximation for the initial conditions $G_1(0) = (0, 0, 1)$ and $G_2(0) = (0, 0, -1)$: $G'_{1,2}(0)$ are parallel to the *y* axis; $\Gamma_1 = -\Gamma_2 = 1$. (*a*) For $\alpha_{1,2} = 1$; the arrows in the inset are the $G''_1(\eta)$ vectors, depicting the helicity of the filament. (*b*) For $\alpha_{1,2} = 10$; the filaments have a higher radius of curvature and are starting to resemble straight lines.

Of course, although self-similar solutions for filament shape are a reasonable expectation for the dynamics near a singular event, it is not the only possibility; there could, for example, be oscillations as the singularity is approached (Pumir, Shraiman & Siggia 1992; Pomeau & Sciamarella 2005). Here we present a generalization of our argument for singular events that are not self-similar and demonstrate that there is still necessarily an antagonistic connection between the stretching exponent *p* and filament curvature; in particular, *p* will not asymptotically vanish only if the length scale characterizing filament curvature is asymptotically different from $\sqrt{\Gamma(t^* - t)}$.

We consider that the solution near the collapse is given by a time-dependent generalization of (4.1), $G(\eta, \tau)$ with $\tau = -\log(t^* - t)$. Substituting into the governing equation results in the following partial differential equation:

$$G_\tau - \tfrac{1}{2}(G - \eta G_\eta) \approx c\tau G_\eta \times G_{\eta\eta} + F[G], \tag{6.1}$$

where the prefactor $c\tau$ (with *c* a constant) to the $G_\eta \times G_{\eta\eta}$ term arises from the binormal law, assuming that the core radius decreases asymptotically faster than the filament curvature. We have used approximate equality (similar to (5.1)) to emphasize that rescaling the velocity on the left-hand side to real space captures the velocity of the corresponding point on the filament at fixed arclength *s*. To follow a Lagrangian marker α along the filament, the tangential stretching term, $[(t^* - t)/l(t)]s_t(\alpha, t)G_\eta$, should be added to the left-hand side resulting in an equality.

The stretching rate of $\boldsymbol{G}$ is evaluated as before using the velocity field on the right-hand side of (6.1). Define the separation distance between Lagrangian markers β on the filament in similarity space as $l(\beta, \tau_0) = |\boldsymbol{G}_\eta(\eta, \tau_0)|$, where $\eta(\beta, \tau_0) = \beta$; then

$$\frac{l_\tau}{l} = \frac{1}{\eta_\beta} \frac{\mathrm{d}\eta_\beta}{\mathrm{d}\tau}. \tag{6.2}$$

Plugging the independent scaling law for the stretching of the core $(t^* - t)^p$ into the real-space stretching s_α (2.5) yields

$$p = \frac{1}{\eta_\beta} \frac{\mathrm{d}\eta_\beta}{\mathrm{d}\tau} = \frac{\mathrm{d}F[\boldsymbol{G}]}{\mathrm{d}\eta} \cdot \boldsymbol{G}_\eta. \tag{6.3}$$

As above, for a self-consistent collapse we must have $p(\eta) > 1$ for all finite η in the limit $\tau \to \infty$.

To see how the dynamics of the curvature of filaments in similarity space (denoted with a bar, so as not to be confused with real-space curvature κ) $\bar{\kappa} = |\mathrm{d}^2\boldsymbol{G}/\mathrm{d}\eta^2|$ is coupled to stretching, we follow β instead of η, since its partial derivative commutes with that of τ (see e.g. Nakayama, Segur & Wadati 1992; Goldstein & Langer 1995):

$$\bar{\kappa}_\tau = \frac{\mathrm{d}}{\mathrm{d}\tau} \left(\beta_\eta^2 \frac{\mathrm{d}^2\boldsymbol{G}}{\mathrm{d}\beta^2} + \beta_{\eta\eta} \frac{\mathrm{d}\boldsymbol{G}}{\mathrm{d}\beta} \right) \cdot \boldsymbol{n}, \tag{6.4}$$

where $\boldsymbol{n}$ is the unit vector along $\mathrm{d}^2\boldsymbol{G}/\mathrm{d}\eta^2$. With some algebra, we obtain

$$\bar{\kappa}_\tau = \left(\frac{\mathrm{d}^2\boldsymbol{G}_\tau}{\mathrm{d}\eta^2} - 2\beta_\eta^2 \frac{\mathrm{d}^2\boldsymbol{G}}{\mathrm{d}\beta^2} \frac{\mathrm{d}\eta_\beta/\mathrm{d}\tau}{\eta_\beta} \right) \cdot \boldsymbol{n}, \tag{6.5}$$

where $(\mathrm{d}\eta_\beta/\mathrm{d}\tau)/\eta_\beta$ is simply the stretching and given by (6.2), so

$$\bar{\kappa}_\tau = \frac{\mathrm{d}^2\boldsymbol{G}_\tau}{\mathrm{d}\eta^2} \cdot \boldsymbol{n} - 2\bar{\kappa} \frac{\mathrm{d}F[\boldsymbol{G}]}{\mathrm{d}\eta} \cdot \boldsymbol{t}. \tag{6.6}$$

Equation (6.3) then simplifies this to

$$\bar{\kappa}_\tau = \frac{\mathrm{d}^2\boldsymbol{G}_\tau}{\mathrm{d}\eta^2} \cdot \boldsymbol{n} - 2p\bar{\kappa}. \tag{6.7}$$

The above equation establishes an intrinsic connection between stretching and dynamics of curvature. If the first term on the right-hand side is dominant, $\bar{\kappa}$ becomes singular or vanishes at finite τ, which is inconsistent with the assumption of a singularity at the limit $\tau \to \infty$. If the second term on the right-hand side dominates, and if p approaches a non-zero constant as $\tau \to \infty$, then the filament curvature $\bar{\kappa}$ decays exponentially in τ. In real space, this implies that the filament radius of curvature would obey a different scaling law than the $\sqrt{\Gamma(t^* - t)}$ suggested by dimensional analysis. In contrast, if $p \to 0$ as $\tau \to \infty$, e.g. like the $p \sim 1/\tau$ demonstrated in the self-similar solution, the scaling laws are preserved up to logarithmic corrections but filament stretching is not fast enough for the solution to be asymptotically self-consistent.

The only way that this conundrum can be avoided is if p asymptotes to a constant larger than 1, and that the right-hand side of (6.7) balances in the asymptotic limit, so that $(\mathrm{d}^2\boldsymbol{G}_\tau/\mathrm{d}\eta^2) \cdot \bar{\boldsymbol{n}} = 2p\bar{\kappa} + f(\tau)$, where $f(\tau)$ can be a polynomial function of τ, and $(\mathrm{d}^2\boldsymbol{G}_\tau/\mathrm{d}\eta^2)$ follows from (6.1). Although we are not able to prove that such an exact balance is impossible, it seems to us unlikely that it could occur; there will be two

restrictions that must be satisfied at every point on the filament, the above balance and also $p > 1$. But since each filament only has two degrees of freedom (i.e. curvature and torsion), this is highly restrictive and cannot be generally satisfied.

7. Conclusions

We have developed a theoretical description of the collapse of interacting vortex filaments, based on an ansatz of asymptotic solutions comprising filament shapes that follow the scaling law set by dimensional analysis, and are weakly coupled to a core with an arbitrary scaling law. We first applied this approach to the case of two filaments, neglecting explicit time dependence. In all possible asymptotic geometries, filament shapes slowly (logarithmically) straighten as they approach the singularity, eliminating the tangential stretching due to interactions. This implies that the core can never shrink fast enough to keep up with the collapse for any initial conditions. A generalization to non-self-similar solutions explicitly illustrates the difficulty of inducing self-consistent singular stretching without violating the scaling law set by the dimension of circulation.

Although the approach outlined herein has failed to construct an explicit singular solution of the Euler equation, the solutions we have described give the appropriate outer solution for the shape of vortex filaments, suitable for characterizing their stretching and distortion before vortex reconnection. We plan on reporting on these solutions in a future work.

Acknowledgements

Supplementary material

Supplementary materials are available at http://dx.doi.org/10.1017/jfm.2012.270.

REFERENCES

AREF, H. 1979 Motion of three vortices. *Phys. Fluids* **22**, 393–400.

BEALE, J., KATO, T. & MAJDA, A. 1984 Remarks on the breakdown of smooth solutions for the 3-D Euler equations. *Commun. Math. Phys.* **94**, 61–66.

CHAE, D. 2007 Nonexistence of self-similar singularities for the 3d incompressible Euler equations. *Commun. Math. Phys.* **273**, 203–215.

CHAE, D. 2010 On the generalized self-similar singularities for the Euler and the Navier–Stokes equations. *J. Funct. Anal.* **258**, 2865–2883.

CHILDRESS, S. 2008 Growth of anti-parallel vorticity in Euler flows. *Physica* D: *Nonlinear Phenomena* **237**, 1921–1925.

CONSTANTIN, P. 2008 Singular, weak and absent: solutions of the Euler equations. *Physica* D: *Nonlinear Phenomena* **237**, 1926–1931.

CONSTANTIN, P., FEFFERMAN, C. & MAJDA, A. 1996 Geometric constraints on potentially singular solutions for the 3-D Euler equations. *Commun. Part. Diff. Equ.* **21**, 559–571.

DENG, J., HOU, T. & YU, X. 2006 Improved geometric conditions for non-blowup of the 3D incompressible Euler equation. *Commun. Part. Diff. Equ.* **31**, 293–306.

EGGERS, J. & FONTELOS, A. 2009 The role of self-similarity in singularities of partial differential equations. *Nonlinearity* **22**, R1–R44.

GIBBON, J. 2008 The three-dimensional Euler equations: Where do we stand? *Physica* D: *Nonlinear Phenomena* **237**, 1894–1904.

GOLDSTEIN, R. E. & LANGER, S. 1995 Nonlinear dynamics of stiff polymers. *Phys. Rev. Lett.* **75**, 1094–1097.

GUTIERREZ, S., RIVAS, J. & VEGA, L. 2003 Formation of singularities and self-similar vortex motion under the localized induction approximation. *Commun. Part. Diff. Equ.* **28**, 927–968.

HOU, T. Y. & LI, R. 2006 Dynamic depletion of vortex stretching and non-blowup of the 3-D incompressible Euler equations. *J. Nonlinear Sci.* **16**, 639–664.

KERR, R. 1993 Evidence for a singularity of the three-dimensional, incompressible Euler equations. *Phys. Fluids* A: *Fluid Dynamics* **5**, 1725–1746.

KIMURA, Y. 2010 Self-similar collapse of 2D and 3D vortex filament models. *Theor. Comput. Fluid Dyn.* **24**, 389–394.

KLEIN, R. & MAJDA, A. 1993 An asymptotic theory for the nonlinear instability of antiparallel pairs of vortex filaments. *Phys. Fluids* A: *Fluid Dynamics* **5**, 369–379.

KLEIN, R., MAJDA, A. & DAMODARAN, K. 1995 Simplified equations for the interaction of nearly parallel vortex filaments. *J. Fluid Mech.* **288**, 201–248.

LERAY, J. 1934 On the motion of a viscous liquid filling space. *Acta Mathematica* **63**, 193–248.

MAJDA, A. & BERTOZZI, A. L. 2001 *Vorticity and Incompressible Flow*. Cambridge University Press.

MEIRON, D., ORSZAG, S., NICKEL, B., MORF, R. & FRISCH, U. 1983 Small-scale structure of the Taylor–Green vortex. *J. Fluid Mech.* **130**, 411–452.

MOFFATT, H. 2000 The interaction of skewed vortex pairs: a model for blow-up of the Navier–Stokes equations. *J. Fluid Mech.* **49**, 51–68.

MORF, R., ORSZAG, S. & FRISCH, U. 1980 Spontaneous singularity in three-dimensional inviscid, incompressible flow. *Phys. Rev. Lett.* **44**, 572–575.

NAKAYAMA, K., SEGUR, H. & WADATI, M. 1992 Integrability and the motion of curves. *Phys. Rev. Lett.* **69**, 2603–2606.

PAOLETTI, M. S., FISHER, M. E. & LATHROP, D. P. 2010 Reconnection dynamics for quantized vortices. *Physica* D: *Nonlinear Phenomena* **239**, 1367–1377.

PAOLETTI, M. S., FISHER, M. E., SREENIVASAN, K. R. & LATHROP, D. P. 2008 Velocity statistics distinguish quantum turbulence from classical turbulence. *Phys. Rev. Lett.* **101**, 154501.

PELZ, R. 1997 Locally self-similar, finite-time collapse in a high-symmetry vortex filament model. *Phys. Rev.* **55**, 1617–1626.

POMEAU, Y. & SCIAMARELLA, D. 2005 An unfinished tale of nonlinear PDEs: Do solutions of 3D incompressible Euler equations blow-up in finite time? *Physica* D: *Nonlinear Phenomena* **205**, 215–221.

PUMIR, A., SHRAIMAN, B. I. & SIGGIA, E. 1992 Vortex morphology and Kelvin's theorem. *Phys. Rev.* **45**, R5351–R5354.

PUMIR, A. & SIGGIA, E. 1987 Vortex dynamics and the existence of solutions to the Navier–Stokes equations. *Phys. Fluids* **30**, 1606–1626.

PUMIR, A. & SIGGIA, E. 1990 Collapsing solutions to the 3-D Euler equations. *Phys. Fluids* A: *Fluid Dynamics* **2**, 220–241.

SAFFMAN, P. G. 1992 *Vortex Dynamics*. Cambridge University Press.

SAFFMAN, P. & BAKER, G. 1979 Vortex interactions. *Annu. Rev. Fluid Mech.* **11**, 95–122.

SCHWARZ, K. W. 1985 Three-dimensional vortex dynamics in superfluid ^{4}He: line–line and line–boundary interactions. *Phys. Rev.* **31**, 5782–5804.

SIGGIA, E. 1985 Collapse and amplification of a vortex filament. *Phys. Fluids* **28**, 794–805.

TAYLOR, G. & GREEN, A. 1937 Mechanism of the production of small eddies from large ones. *Proc. R. Soc. Lond.* **158**, 499–521.

DE WAELE, A. & AARTS, R. 1994 Route to vortex reconnection. *Phys. Rev. Lett.* **72**, 482–485.